

A self-consistent theory for graphene transport

Shaffique Adam[†], E. H. Hwang, V. M. Galitski, and S. Das Sarma

Condensed Matter Theory Center, Department of Physics, University of Maryland, College Park, MD 20742-4111

Edited by Ellen D. Williams, University of Maryland, College Park, MD, and approved October 1, 2007 (received for review May 23, 2007)

We demonstrate theoretically that most of the observed transport properties of graphene sheets at zero magnetic field can be explained by scattering from charged impurities. We find that, contrary to common perception, these properties are not universal but depend on the concentration of charged impurities n_{imp} . For dirty samples ($250 \times 10^{10} \text{ cm}^{-2} < n_{\text{imp}} < 400 \times 10^{10} \text{ cm}^{-2}$), the value of the minimum conductivity at low carrier density is indeed $4e^2/h$ in agreement with early experiments, with weak dependence on impurity concentration. For cleaner samples, we predict that the minimum conductivity depends strongly on n_{imp} , increasing to $8e^2/h$ for $n_{\text{imp}} \approx 20 \times 10^{10} \text{ cm}^{-2}$. A clear strategy to improve graphene mobility is to eliminate charged impurities or use a substrate with a larger dielectric constant.

Boltzmann transport | electron transport | minimum conductivity

The past two years have seen a proliferation of theoretical and experimental interest in graphene. The interest stems mainly from the striking differences between graphene and other more well known semiconductor-based 2D systems that arise mostly from its unique band structure, which is obtained by considering graphene to be a single sheet of carbon atoms arranged in a honeycomb lattice. Graphene is in fact a carbon nanotube rolled out into a single 2D sheet, and as is already known from the study of carbon nanotubes, electrons moving in the periodic potential generated by the carbon lattice form a band that displays striking properties, such as having a chiral Dirac equation of motion with a mathematical structure similar to Weyl neutrinos. This intriguing “relativistic” Dirac–Weyl spectrum of graphene has attracted substantial interest and attention. Although this analogy of considering graphene as a solid-state realization of the “massless chiral Dirac Fermion” model (developed as a solution to Dirac’s Lorentz invariant generalization of Schrödinger’s equation) has some utility, it also has the potential to be misleading. In particular, as we argue here, searching to explain the experimental transport properties of graphene by focusing on the “Dirac point” (see the formal definition below) obscures the real mechanism of carrier transport. In this respect, and from our perspective, the physics of graphene has more in common with the metal oxide-semiconductor-field effect transistors (MOSFETs) that form the backbone of our current semiconductor industry than with the physics of relativistic chiral Fermions. Studying graphene is therefore as much about making useful MOSFETs from pencil smudges, as it is about studying quantum electrodynamics in a pencil mark.

We observe that already within one year since the fabrication of the first gated 2D graphene samples (that enable a variable external gate voltage-tuned carrier density), mobilities as high as $2.5 \text{ m}^2/\text{V s}$ have been reported, and these values are comparable to the best Si MOSFET samples at low temperature. In addition, graphene mobility is relatively temperature-independent, making room-temperature 2D graphene mobilities to be among the highest in field effect transistor-type devices. It is therefore both of fundamental and technological interest to understand the transport mechanism in graphene in reasonable qualitative and quantitative detail. Similar to MOSFETs, transport properties of graphene are determined by scattering from charged impurities that invariably are present. We report here the essential graphene transport theory focusing on charged impurity scattering.

Before this work, the conventional wisdom in the graphene community was that close to the Dirac point, carrier transport is ballistic, that the minimum conductivity is universal, and that we lack a basic understanding of how at the Dirac point there could be carrier-free transport over micrometer-sized distances. In this context, our work provides a theoretically simple explanation for this graphene transport mystery: charged impurities in the substrate generate carrier density fluctuations that allow for nonuniversal diffusive transport, and these density inhomogeneities render the Dirac point physics experimentally inaccessible, at least for current graphene samples (see *Note*).

We emphasize that, although the importance of charged impurity scattering in determining the linear-in-density high-density (i.e., far from the charge-neutral Dirac point) graphene carrier transport has already been established (1–4) in the literature, the current work points out that the same charged impurities will have a qualitative effect at low carrier density close to the Dirac point by providing an inhomogeneous electron-hole puddle landscape where the conductivity will be approximately a constant over a finite range of external gate voltage, providing a simple and physically appealing explanation for the observed graphene minimum conductivity plateau. The importance of our work, therefore, lies in its ability to explain the graphene transport data at low carrier density through a physically appealing charged impurity-induced mechanism that quantitatively explains both the existence (and the width) of the minimum conductivity plateau as well as its magnitude. Up to now, in the literature, the minimum conductivity phenomenon in graphene was considered to be an outstanding experimental puzzle.

In this context, “bare graphene” is the empty honeycomb lattice, where allowing for electron hopping between adjacent sites gives the linear Dirac–Weyl spectrum. The nominally undoped or ungated situation is that the completely filled valence band and a completely empty conduction band touch at the Dirac point, making graphene a zero-gap semiconductor. The Dirac point is a singular point of measure zero that separates the conduction and the valence band in the linear graphene spectrum. This “intrinsic graphene” with the chemical potential (or Fermi energy) precisely at the Dirac point has no free carriers and is obviously an abstract model, because the slightest amount of doping or external potential will induce carriers in the system. Charged impurity disorder or spatial inhomogeneity will render this intrinsic graphene experimentally unrealizable. “Extrinsic graphene” is when one induces free carriers (either electrons in the conduction band with a positive potential, or holes in the valence band with a negative potential), by applying an external gate voltage V_g , or equivalently, by doping the system. Carrier bands are filled up to a certain Fermi energy, E_F , determined by the electrostatic potential configura-

Author contributions: S.A., E.H.H., V.M.G., and S.D.S. designed research; S.A., E.H.H., V.M.G., and S.D.S. performed research; and S.A. and S.D.S. wrote the paper.

The authors declare no conflict of interest.

This article is a PNAS Direct Submission.

Abbreviations: MOSFET, metal oxide-semiconductor-field effect transistor; RPA, random phase approximation.

[†]To whom correspondence should be addressed. E-mail: adam1@umd.edu.

© 2007 by The National Academy of Sciences of the USA

tion of the graphene environment and, depending on which is larger, could be dominated either by the external gate voltage or by charged impurities. All experimental graphene samples are extrinsic, because there are invariably some free carriers present in the system, and transport close to the Dirac point is dominated by two distinct effects of the charged impurities in the system: (i) the induced graphene carrier density is self-consistently determined by the screened, charged impurity potential, and (ii) the conductivity is determined by charged impurity scattering.

As one would expect with any newly discovered electronic material (5), the full gamut of experimental techniques has been used to explore graphene properties, including light scattering (6), angle-resolved photoemission spectroscopy (7), and surface probe measurements (8, 9). The field continues to evolve with new ideas being explored, including making suspended graphene (10) and electromechanical resonators (11), transfer-printing graphene onto plastic (12), using superconducting (13) and ferromagnetic leads (14), having patterned top gates (15–17), exposing samples to molecular dopants (18), and fabricating graphene nano-ribbons (19). These rapid experimental advances show that the study of graphene is still in its infancy, with many promises for the discovery of new physics and application to technology.

The focus of the present work is on the important graphene transport measurements (20, 21). These were the first experiments to be done and are still not understood, in that there are widely disparate claims on the transport mechanism. Because these experiments form the basis for most of the future work on graphene as well as its prospective technological applications, a correct understanding of the basic transport physics is of fundamental importance. Although many features are observed in the transport experiments, two have been highlighted and particularly discussed in the literature, namely, the low-density “minimum conductivity” σ_0 , that is, the value of the conductivity at or near the Dirac point (where $E_F \approx 0$, and a naïve picture would suggest that there are no charge carriers); and the high-density conductivity $\sigma(n)$, which is linear in the carrier density n , giving a constant mobility $\mu = \sigma/ne$. As we discuss below, our analytic theory explains both features quantitatively and makes predictions for the width of the minimum conductivity plateau and the offset of the Dirac point from zero-gate voltage.

In the literature, most theoretical work has focused on the short-range scattering mechanism (also called “white noise” disorder) to understand graphene transport, mainly as a matter of technical convenience. Early work using a Kubo formalism in the ballistic limit (22, 23) showed that the conductivity for massless Dirac Fermions is $e^2/(\pi h)$ for vanishing disorder, and that this universal value occurs only at the Dirac point and not in its vicinity. At finite carrier density, the Kubo formalism with short-range scattering gives a conductivity that is constant with carrier density (1) and not the linear-in-density behavior seen in experiments. Certain numerical (2) and analytic (24) methods that try to extrapolate between these two limits inevitably get a square-root dependence of conductivity on density (not linear) and give orders-of-magnitude incorrect values for the mobility. More recently, short-range scattering has been considered theoretically (25–27) with the finding that, at zero temperature, localization effects should give $\sigma_0 = 0$. Although all these works improve our abstract theoretical understanding of graphene, they are all in qualitative disagreement with existing experimental data. We argue here that short-range scattering has little to do with the experiments of Refs. 5, 20, and 21, and that, although localization effects may very well be important in the zero-temperature limit, the existing bulk graphene transport data at accessible temperatures ($T > 0.1$ K) are in the Drude–Boltzmann diffusive transport regime. Equally important, the observed transport properties of doped graphene do not access the Dirac point physics, at least in the currently available samples (20, 21), which have fairly large concentrations of charged impurity

centers. Although the observed conductivity value (and not conductance) of $4e^2/h$ in dirty samples brings to mind connections with universal conductance quantization phenomena such as 1D point-contact conductance quantization or Zitterbewegung or quantized Hall resistance, we argue here that no such universal physics is at play in current bulk graphene transport experiments where conductivity, and not conductance is being discussed. Our goal here is to develop a quantitatively accurate analytic theory for the most important graphene transport problem, namely, the regular bulk dc conductivity studied in the diffusive Drude–Boltzmann limit, which is the regime of technological interest. We argue that charged impurity scattering is responsible for most of the observed bulk diffusive transport behavior in graphene. Charged impurities could reside either inside the substrate or be created near the graphene–substrate interface during the processing and handling of samples. The typical concentration of charged impurities in a SiO₂ substrate is $n_{\text{imp}} \approx 50 \times 10^{10} \text{ cm}^{-2}$ and is known to dominate the transport properties of other extensively studied 2D semiconductor systems (28).

Earlier work (2–4) demonstrated that, although the mean free path for short-range scatterers $\ell_s \sim 1/\sqrt{n}$, where n is the carrier density, for Coulomb (i.e., charged impurity) scatterers $\ell_c \sim \sqrt{n}$. This finding implies that, although graphene at low density is a clean or ballistic system for short-range scatterers, it is a dirty and diffusive system for long-range scatterers. At low carrier densities of $n \approx n_{\text{imp}} \approx 50 \times 10^{10} \text{ cm}^{-2}$, one can estimate that $\ell_s \geq 1,000 \text{ nm}$ and $\ell_c \lesssim 50 \text{ nm}$. Therefore, at the lowest densities close to the Dirac point, graphene transport properties are completely dominated by Coulomb scattering. This simple argument also establishes that any short-range scattering, even if it is present in graphene, is irrelevant in the low carrier density limit near the Dirac point where the minimum conductivity plateau is observed.

In the present work we provide a complete picture of transport in both high and low carrier density regimes by using a self-consistent random phase approximation (RPA)–Boltzmann formalism where the impurity scattering by the charged carriers themselves is treated self-consistently in the RPA, and the dc conductivity is calculated in the Boltzmann kinetic theory. We derive analytic expressions for (i) mobility μ , (ii) plateau width, (iii) minimum conductivity, and (iv) shift in gate voltage. Our results for graphene on a SiO₂ substrate can be summarized as

$$\sigma(n - \bar{n}) = \begin{cases} \frac{20e^2 n^*}{h n_{\text{imp}}} & \text{if } n - \bar{n} < n^* \\ \frac{20e^2 n}{h n_{\text{imp}}} & \text{if } n - \bar{n} > n^* \end{cases}, \quad [1]$$

where Eq. 10 below gives analytic expressions for n^* and \bar{n} .

An important finding of our work is that for dirty samples with $n_{\text{imp}} \approx 3.5 \times 10^{12} \text{ cm}^{-2}$, σ_0 is indeed close to $4e^2/h$ as observed experimentally, and not very sensitive to changes in disorder, whereas for cleaner samples with $n_{\text{imp}} \approx 2 \times 10^{11} \text{ cm}^{-2}$, $\sigma_0 \approx 8e^2/h$, and is sensitive to the value of n_{imp} , thus explaining the mystery of why more recent experiments show a larger magnitude and larger spread in the value of σ_0 . For the typical densities used in the early graphene experiments, the minimum conductivity appears to saturate at a universal value of $4e^2/h$, but we predict that there is nothing universal here, and for dirtier samples, the value of the minimum conductivity as a function of n_{imp} would slowly decrease.

The formalism developed here to obtain Eq. 1 can be divided into three steps. First, we develop an analytic solution for the Boltzmann transport theory by using the full RPA treatment of the charged impurity scattering. We find analytically that $\sigma \approx 20(e^2/h)(n/n_{\text{imp}})$ in agreement with earlier numerical calculations

(2–4). Second, we extend the methods of Refs. 29 and 30 to evaluate the screened voltage fluctuations induced by charged impurities. Here, we calculate the potential fluctuations by using the full RPA screening, which, although being complicated and cumbersome, is necessary to obtain quantitative agreement. Third, we develop a theory to calculate the residual carrier density n^* self-consistently. We find that the ratio n^*/n_{imp} , which is directly related to the minimum conductivity through $\sigma_0 \approx 20(e^2/h)(n^*/n_{\text{imp}})$, is a monotonically decreasing function of n_{imp} and the dependence gets weaker for larger impurity density.

Before we provide details of our calculation, we first address the range of validity of our self-consistent RPA–Boltzmann theory. First, we consider only Coulomb scattering. As already discussed (see also ref. 4), other scattering mechanisms are irrelevant at low density, and the experimentally observed linear dependence of conductivity with carrier density singles out charged impurities as the dominant scattering mechanism. Only in the limit of very small charged impurity density, must one include short-range scattering into the formalism (such short-range scattering may arise from point defects and dislocations in the lattice). We find $\sigma_0 = (4e^2/h)[n_{\text{imp}}/(5n^*) + \eta]^{-1}$, where we estimate $\eta = 2/k_F \ell_s \lesssim 1/10$, suggesting that for very low impurity densities (two orders of magnitude lower n_{imp} than present day samples), σ_0 will saturate at $\approx 20e^2/h$, before our charged impurity model gives way to short-range scattering. Second, our theoretical calculation is done at zero temperature. Theoretically, one expects (3) very weak temperature dependence for $T \ll T_F$, and this is indeed consistent with experimental observations where $T/T_F \lesssim 0.2$. Third, because the sample sizes are several microns in length, and the mean free path is tens of nanometers, we are certainly in the diffusive as opposed to the ballistic transport regime. Fourth, electron interactions are treated within the RPA scheme. RPA is an expansion in r_s , and in graphene experiments on SiO_2 , $r_s \approx 0.8$, so one would expect it to work better than for 2D semiconductors or metals, where, although $r_s \approx 2$ –10, RPA provides an excellent approximation. Fifth, the scattering time is calculated by using Boltzmann kinetic theory. Formally, Boltzmann theory (as described by Eq. 3 below) is valid for $k_F \ell \gg 1$, but it is also the standard theory used to describe Coulomb scatterers in 2D systems (28, 31). For clean graphene samples, $k_F \ell \approx 4$ at low density and $k_F \ell \approx 100$ at high density, making the Boltzmann theory valid. Sixth, the average carrier density is obtained from the potential fluctuations by using a local density (also called Thomas–Fermi) approximation as is normally done in 2D systems (29, 32). This is valid so long as $n^*/n_{\text{imp}} \gg 0.01$, which guarantees that the spacing between electrons is much less than the length of the conducting cluster (33). This local density condition holds both empirically and is established *a posteriori* to be valid throughout the Boltzmann transport regime. Similarly, this argument demonstrates that in current experiments the Dirac cone is always filled with electrons or holes whose average density ranges from $0.2 n_{\text{imp}}$ to $0.5 n_{\text{imp}}$. Formally, one can consider the limit $n_{\text{imp}} \rightarrow \infty$ and find that $n^* = (n_{\text{imp}}/32d^2\pi)^{1/2}$, with no lower bound on the minimum conductivity $\sigma_0 \sim 1/\sqrt{n_{\text{imp}}}$, but this “mean-field” approximation breaks down when the inhomogeneities become so large that calculating the conductivity through the Boltzmann transport of the average density n^* becomes meaningless. Seventh, we ignore the Anderson localization. The observed experimental absence of Anderson localization is not unique to graphene. In 2D semiconductor systems (34–36), a percolation metal–insulator transition is seen at low carrier densities instead of a localization transition, whereas in graphene the percolation transition is an electron–metal to hole–metal transition without any intervening insulating phase. Moreover, recent numerical work (37, 38) suggests that there may not be a metal–insulator transition in graphene. Naturally, one could relax any of the assumptions above in a future calculation, but for the purpose of

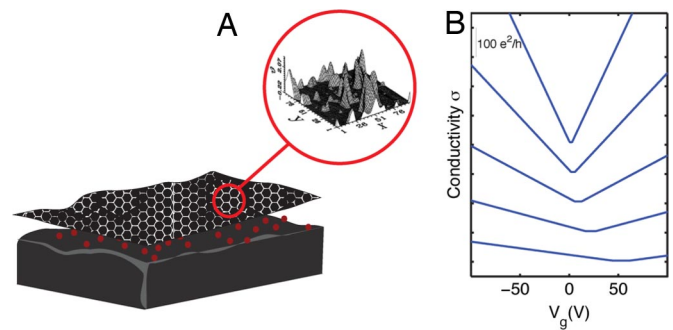


Fig. 1. Schematic of graphene transport properties. (A) Shown is a cartoon of our model where charged impurities in the substrate at a distance d away from the graphene sheet create a spatially inhomogeneous screened Coulomb potential. At low carrier density, the system breaks up into puddles of electrons and holes. The residual density is then calculated self-consistently, giving remarkable agreement with experimental results. (Inset) This graphic (taken from ref. 29) is used here just to illustrate the voltage fluctuations schematically, where it is understood that the presence of both electron and hole carriers implies that both positive and negative voltages are screened. (B) Predicted conductivity traces (Eq. 1) for different values of n_{imp} . Curves are offset vertically by $100e^2/h$ for clarity and show, from top to bottom, impurity concentrations (in units of 10^{10} cm^{-2}): 20 (very clean), 40, 80, 160, 320 (very dirty). Most of the samples considered in ref. 20 had mobilities between the bottom two curves. Clearly seen are the gate voltage offset V_g^D and the minimum conductivity plateau, which are larger for the dirtier samples.

comparison with current graphene experiments, these approximations are well justified and provide a consistent framework to understand graphene transport. We observe that, in our RPA–Boltzmann theory, σ_0 reaches the so-called universal Dirac point minimum conductivity value (22, 23, 39) of $e^2/(\pi\hbar)$ for unphysically large-impurity densities of $n_{\text{imp}} \gtrsim 10^{14} \text{ cm}^{-2}$, where the diffusive transport approximation no longer applies.

The theoretical picture presented here is shown heuristically in Fig. 1. Charged impurities either in the substrate or in the vicinity of graphene create a spatially inhomogeneous potential distribution in the graphene plane. At low carrier density, the spatially inhomogeneous potential breaks the system up into puddles of electrons and holes. This theoretical prediction (4) has now been verified in a recent surface probe experiment (9) by using a scanning single-electron transistor to directly measure the potential fluctuations in graphene, and by finding quantitative agreement with earlier predictions (30) for the height and width of the electron and hole puddles. In addition, there is recent indirect experimental support (16, 17) for the electron–hole puddle picture proposed in ref. 4. Unlike the usual 2D systems, both electrons and holes screen the external potential. These potential fluctuations directly change the local chemical potential, inducing a residual density that in turn changes the screening. Here, we use a self-consistent procedure to determine the residual density n^* , which manifests itself in experiments by a residual conductivity plateau that is shifted by an offset gate voltage $V_g^D = \bar{n}/\alpha$, whose width is n^* and whose magnitude is $\sigma(n^*)$, where $\sigma(n)$ is the RPA–Boltzmann conductivity for carrier density n . V_g^D is called the Dirac gate voltage because it is the value of the external gate voltage where the Hall coefficient changes sign, indicating that carriers change from electrons to holes. In MOSFETs, the voltage corresponding to V_g^D is often referred to as the “threshold voltage,” because in these systems it marks the onset of conductivity at this critical value of carrier density, and $\sigma = 0$ below this threshold. In graphene, V_g^D separates the conducting electron and conducting hole transport regimes, whereas in MOSFETs the threshold voltage separates conducting and insulating 2D channels. Here, $\alpha \approx 7.2 \times 10^{10} \text{ cm}^{-2} \text{ V}^{-1}$ is a geometry-related factor [which can be measured

directly (20, 21) by using Hall measurements] and is used to convert the experimentally measured gate voltage to carrier density n . For the rest of the article, we develop the theory only for carrier density $n = k_F^2/\pi$, where it is understood that any comparison with the experimentally measured gate voltages is made by using $n = \alpha V_g$.

Based on estimates from surface probe measurements (5, 8), and consistent with earlier work both in graphene (4, 30) and in Si MOSFETs (28, 40), we assume that the charged impurities lie in a plane at a distance $d \approx 1$ nm from the graphene sheet and calculate the voltage fluctuations taking into account the screening by using the RPA. The screened voltage fluctuation is a function of d and the carrier density n ; a larger carrier density more effectively screens the charged impurities, whereas the potential fluctuations are larger for low carrier density. We include this effect self-consistently in our theory, where n both is determined by and determines the screened impurity potential. Our theoretical results do not depend in any qualitative manner on the precise choice of d , and one can develop relationships between the four experimental quantities (i.e., mobility, plateau width, minimum conductivity, and shift in gate voltage) that are independent of d . We emphasize that, because a single parameter n_{imp} determines all four experimental quantities, we anticipate that our theory would be consistent with each of them to within a factor of 2. Comparison with representative samples from the Columbia, Manchester, and Maryland groups (see Fig. 3 *Inset* and *Note*) shows good agreement for the mobility and gate-voltage shift and agrees to within the expected factor of 2 with measurements of the plateau width and minimum conductivity. We now proceed to calculate the Boltzmann transport conductivity. For 2D graphene, the semiclassical diffusivity is given by

$$\sigma = \frac{g_s g_v e^2 E_F \tau}{h 2\hbar} = \frac{g_s g_v e^2 k_F \ell}{h 2\hbar}, \quad [2]$$

where $g_s = g_v = 2$ are the spin and valley degeneracy factors and the mean free path $\ell = v_F \tau$, with the scattering time τ being given at $T = 0$ by

$$\frac{\hbar}{\tau(\mathbf{k})} = \frac{n_{\text{imp}}}{4\pi} \int d\mathbf{k}' \left[\frac{V(|\mathbf{k}-\mathbf{k}'|)}{\varepsilon(|\mathbf{k}-\mathbf{k}'|)} \right]^2 [1 - \cos^2(\theta)] \delta(E_{\mathbf{k}'} - E_{\mathbf{k}}), \quad [3]$$

where $V(q) = 2\pi e^{-qd} e^2/(\kappa q)$ is the Fourier transform of bare Coulomb potential at the transfer momentum $q = |\mathbf{k} - \mathbf{k}'| = 2k_F \sin(\theta/2)$. Although the exact RPA dielectric function is known (41), for our purposes, we can use the following simple approximate expression, which allows for analytic calculations and provides results that are indistinguishable from the exact results (see Fig. 2)

$$\varepsilon(q) = \begin{cases} 1 + q_s/q & \text{if } q < 2k_F, \\ 1 + \pi r_s/2 & \text{if } q > 2k_F, \end{cases} \quad [4]$$

where $q_s = 4 k_F r_s$, and solving the integrals exactly, we find

$$\sigma = \frac{e^2 n}{h n_{\text{imp}} G[2r_s]}, \quad [5]$$

$$\frac{G[x]}{x^2} = \frac{\pi}{4} + 3x - \frac{3\pi x^2}{2} + \frac{x(3x^2 - 2)\arccos[1/x]}{\sqrt{x^2 - 1}},$$

where for graphene on a SiO₂ substrate, $r_s = e^2/(\hbar\gamma\kappa) \approx 0.8$, $G(2r_s) \approx 1/10$, and $\sigma \approx 20 (e^2/h)(n/n_{\text{imp}})$. Note that $G[x]$ is

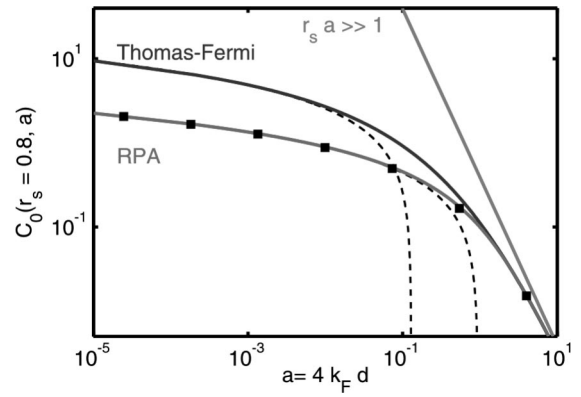


Fig. 2. Comparison of voltage fluctuation $C_0(r_s, a)$ using different screening approximations. The RPA is the main approximation used in the present work. The Thomas–Fermi result was derived in ref. 30 and the “complete screening” result valid for $r_s a \gg 1$, was obtained in ref. 29. All three approximations agree in the large-density limit, but disagree for small density. Shown in dashed lines are small-density analytic asymptotes for the Thomas–Fermi and RPA and squares show the numerical evaluation of Eq. 7 by using the exact dielectric function reported in ref. 41.

positive and real for all x . From this we derive a simple analytic expression for linear tail mobility in graphene:

$$\frac{\mu}{\mu_0} \approx 50 \frac{n_0}{n_{\text{imp}}}, \quad [6]$$

where $\mu_0 = 1m^2/Vs$ and $n_0 = 10^{10} \text{ cm}^{-2}$. Note that Eq. 6 depends only on the charged impurity scattering concentration n_{imp} , indicating that the only way to increase graphene mobility for fixed r_s is to improve the sample quality. However, Eq. 5 also shows that mobility depends on the substrate dielectric constant κ , and therefore, changing the underlying substrate from SiO₂ to a substrate with a higher dielectric constant would reduce r_s , and would be another way to increase sample mobility. For example, changing the substrate to HfO₂ ($\kappa_s \approx 25$) from SiO₂ ($\kappa_s \approx 4$) should enhance graphene mobility by a factor of 5.

We now calculate the statistics of the random voltage fluctuations, significantly extending earlier numerical work (29), to incorporate analytically the nonlinear screening of electrons and holes in a zero-gap situation, to find

$$\overline{\delta V^2} = \overline{[V - V_g^D]^2} = n_{\text{imp}} \int \frac{d^2 q}{(2\pi)^2} \left[\frac{2\pi e^2 e^{-qd}}{\kappa q \varepsilon(q)} \right]^2, \quad [7]$$

$$= 2\pi n_{\text{imp}} \left(\frac{e^2}{\kappa} \right)^2 C_0(r_s, a = 4k_F d),$$

$$C_0^{\text{RPA}}(r_s, a) = -1 + \frac{4E_1(a)}{(2 + \pi r_s)^2} + \frac{2e^{-a} r_s}{1 + 2r_s} + (1 + 2r_s a) e^{2r_s a} (E_1[2r_s a] - E_1[a(1 + 2r_s)]), \quad [8]$$

where the superscript on C_0^{RPA} indicates that we used the RPA, and $E_1(z) = \int_z^\infty t^{-1} e^{-t} dt$ is the exponential integral function. The voltage fluctuation result, $C_0(r_s = 0.8, a)$, is shown in Fig. 2, comparing different approximation schemes used in the literature. The analytic result Eq. 8 is compared with a numerical evaluation of Eq. 7 by using the exact dielectric function first reported in ref. 41, as well as with the long-wavelength (also known as Thomas–Fermi) approximation (30), where $\varepsilon(q) = 1 + q_s/q$ for all q , and the “complete

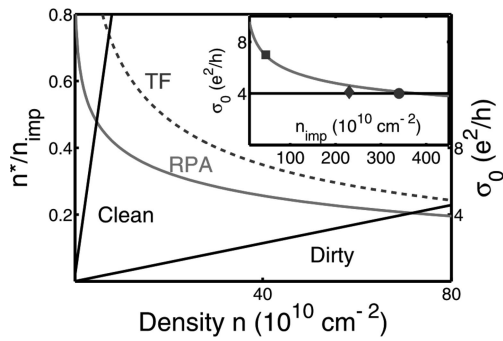


Fig. 3. Shown is Eq. 10. The two lines starting at the origin show n/n_{imp} for $n_{\text{imp}} = 10 \times 10^{10} \text{cm}^{-2}$ (very clean) and $n_{\text{imp}} = 350 \times 10^{10} \text{cm}^{-2}$ (very dirty). The RPA and Thomas–Fermi results show $2r_s^2 C_0(r_s, a = 4d\sqrt{\pi n})$ as a function of carrier density n . The points of intersection represent the self-consistent solution, and one can read off n^* from the x axis, n^*/n_{imp} from the left axis, and the “minimum conductivity” σ_0 from the right axis. (Inset) Shown is σ_0 as a function of charged impurity concentration showing that (i) it is nonuniversal, (ii) dirty samples have $\sigma_0 = 4e^2/h$ over a wide range of impurity concentration, and (iii) the cleanest samples have $\sigma_0 \approx 8e^2/h$, but the value is sensitive to the concentration of charged impurities. Also shown is comparison with representative experimental results from Columbia (square), from Manchester (diamond), and from Maryland (circle). These same three samples (with conductivity shown over the full-density range) were compared with a high-density numerical Boltzmann theory in ref. 4.

screening” approximation (2, 29) that is valid only for $r_s a \gg 1$, where $\varepsilon(q) = q_s/q$. In the limit of large a (i.e., $k_F d \gg 1$), both the Thomas–Fermi and the RPA results approach the complete screening limit of $C_0^{\text{CS}}(r_s, a) = (2r_s a)^{-2}$, which was obtained in ref. 29. The three approximations disagree in the small a (or low-density) limit where

$$C_0^{\text{RPA}}(r_s, a \rightarrow 0) = \frac{-1}{2r_s + 1} - \ln\left[\frac{2r_s}{2r_s + 1}\right] - \frac{4 \ln(\tilde{\gamma} a)}{(2 + \pi r_s)^2}, \quad [9]$$

and $\tilde{\gamma} \approx 1.781$ is Euler’s constant. Notice that for RPA, a combination of the small and large $a = 4k_F d$ asymptotes span most of the density range. Although these analytic asymptotes correctly describe the screened potential for most densities, it turns out that the regime relevant to graphene experiments is the window where they do not work well, and the full functional form of C_0^{RPA} shown in Eq. 8 needs to be used.

As discussed earlier, to determine the self-consistent residual density, we equate the average chemical potential to the fluctuation in the screened, charged impurity-induced potential as $\bar{E}_F^2 = \bar{\delta V}^2$, and find

$$\frac{n^*}{n_{\text{imp}}} = 2r_s^2 C_0^{\text{RPA}}(r_s, a = 4d\sqrt{\pi n^*}), \quad \bar{n} = \frac{n_{\text{imp}}^2}{4n^*}, \quad [10]$$

where the second expression for the impurity-induced shift in voltage is determined from $\bar{V} = \pi n_{\text{imp}} \gamma / (2k_F)$ (29, 30). Combining these results gives Eq 1.

Fig. 3 shows the results of the self-consistent procedure. Fig. 3 Inset shows the value of the minimum conductivity and compares with the experimental results. These are the same three samples that were shown in ref. 4 to compare the conductivity at high carrier density (far from the Dirac point) with a numerical Boltzmann theory, and here we show the low carrier density comparison near the Dirac point. Through Eq. 6, we have the high-density measurements directly giving n_{imp} , and this is the only parameter used to determine the minimum conductivity σ_0 . Our results show that, contrary to common perception, the

graphene minimum conductivity is not universal, but that future cleaner samples will have higher values of σ_0 . We emphasize that, in addition to explaining the value of σ_0 and its dependence on the sample quality, our theory also naturally accounts for the width of the minimum conductivity plateau in agreement with experiments. For example, $n_{\text{imp}} = 350 \times 10^{10} \text{cm}^{-2}$ gives $n^* = 70 \times 10^{10} \text{cm}^{-2}$ and plateau width $\Delta V_g = 10 \text{V}$.

We emphasize that the most important qualitative result of our theory is to introduce a realistic mechanism operational in all disordered graphene samples (i.e., in the presence of random charged impurities) that produce a plateau-like approximate nonuniversal minimum graphene conductivity at low induced carrier density. We obviously cannot rule out other possible “universal mechanisms” that will lead to a “universal” minimum intrinsic graphene conductivity at the Dirac point in the clean limit, a situation beyond the scope of our theory. But the fact that the currently existing experimental data from three different groups exhibit nonuniversal minimum conductivity in approximate (within a factor of 2) agreement with our theory indicates that any intrinsic universal mechanism beyond our model may not yet be playing any role. We note, however, that recent theoretical (39, 42, 43) and experimental (44) work have dealt with ballistic transport in mesoscopic graphene which show universal behavior in the regime where $\ell > W > L$, where ℓ is the mean free path, and W and L are the sample width and length. Our theory does not apply in this zero disorder ballistic limit because our work is built entirely on the picture of diffusive transport through disorder-induced electron-hole puddles.

In summary, we believe we have qualitatively and semiquantitatively solved one of the main transport puzzles in graphene, namely, why the experimentalists see a conductivity minimum plateau and the extent to which this minimum conductivity is or is not universal. The theory developed here should only be taken as a step toward a full quantitative theory of graphene transport, in particular, at the lowest carrier densities. Many questions still remain open, although we believe that we have taken an important step in the right direction. In particular, the precise nature of transport at the charge-neutral Dirac point cannot be accessed by our self-consistent treatment, which is valid only at finite doping away from charge neutrality. Unless there is strong electron-hole tunneling, the percolation through electron and hole puddles becomes precisely equivalent at the Dirac point, and a purely percolative theory, not our self-consistent RPA–Boltzmann theory, would be necessary to understand the transport. We do, however, mention that the observed smooth behavior of conductivity as a function of gate voltage through the charge neutrality point indicates a lack of any dramatic phenomena at the Dirac point, and given that our theory is a good description of transport away from the Dirac point, it is conceivable that it remains quantitatively valid at the charge neutral point also. Given the great deal of current interest in graphene and the potential for graphene-based electronics applications, our transport theory of graphene not only furthers our understanding of this new material, but it provides essential insights on how to obtain higher mobility, which is necessary if graphene is to have serious technological impact as an electronic material.

Note. After submission of this manuscript, there have been two experimental studies (45, 46) that found that our transport theory is in good agreement with experimental data taken over a wide range of charged impurity densities.

We thank M. Fuhrer, A. Geim, P. Kim, and H. Stormer for sharing with us their experimental data. This work is supported by the Office of Naval Research, the Laboratory for Physical Sciences of the National Security Agency, and the National Science Foundation and Nanoelectronics Research Initiative, and the Microsoft Project Q.

1. Ando T (2006) *J Phys Soc Jpn* 75:074716.
2. Nomura K, MacDonald AH (2007) *Phys Rev Lett* 98:076602.
3. Cheianov VV, Fal'ko VI (2006) *Phys Rev Lett* 97:226801.
4. Hwang EH, Adam S, Das Sarma S (2007) *Phys Rev Lett* 98:186806.
5. Novoselov KS, Geim AK, Morozov SV, Jiang D, Zhang Y, Dubonos SV, Grigorieva IV, Firsov AA (2004) *Science* 306:666–669.
6. Yan J, Zhang Y, Kim P, Pinczuk A (2007) *Phys Rev Lett* 98:166802.
7. Bostwick A, Ohta T, Seyller T, Horn K, Rotenberg E (2007) *Nat Phys* 3:36–40.
8. Ishigami M, Chen JH, Cullen WG, Fuhrer MS, Williams ED (2007) *Nano Lett* 7:1643–1648.
9. Martin J, Akerman N, Ulbricht G, Lohmann T, Smet JH, von Klitzing K, Yacobi A (2007) arXiv:0705.2180v1 (cond-mat.mes-hall), preprint.
10. Meyer JC, Geim AK, Katsnelson MI, Novoselov KS, Booth TJ, Roth S (2007) *Nature* 446:60–63.
11. Bunch JS, van der Zande AM, Verbridge SS, Frank IW, Tanenbaum DM, Parpia JM, Craighead HG, McEuen PL (2007) *Science* 315:490–493.
12. Chen JH, Ishigami M, Jang C, Fuhrer MS, Hines D, Williams ED (2007) *Adv Mater*, in press.
13. Heersche HB, Jarillo-Herrero P, Oostinga JB, Vandersypen LMK, Morpurgo AF (2007) *Nature* 446:56–59.
14. Hill EW, Geim AK, Novoselov K, Schedin F, Blake P (2006) *IEEE Trans Magn* 42:2694–2696.
15. Lemme MC, Echtermeyer TJ, Baus M, Kurz H (2007) *IEEE Electron Device Lett* 28:282–284.
16. Huard B, Sulpizio JA, Stander N, Todd K, Yang B, Goldhaber-Gordon D (2007) *Phys Rev Lett* 98:236803.
17. Williams JR, DiCarlo L, Marcus CM (2007) *Science* 317:638–641.
18. Schedin F, Geim AK, Morozov SV, Jiang D, Hill EH, Blake P, Novoselov KS (2007) *Nat Mater* 6:652–655.
19. Han MY, Ozyilmaz B, Zhang Y, Kim P (2007) *Phys Rev Lett* 98(20):206805–206809.
20. Novoselov KS, Geim AK, Morozov SV, Jiang D, Zhang Y, Katsnelson MI, Grigorieva IV, Dubonos SV, Firsov AA (2005) *Nature* 438:197–200.
21. Zhang Y, Tan, Y-W, Stormer HL, Kim P (2005) *Nature* 438:201–204.
22. Fradkin E (1986) *Phys Rev B* 33(5):3257.
23. Ludwig AWW, Fisher MPA, Shankar R, Grinstein G (1994) *Phys Rev B* 50(11):7526–7552.
24. Ziegler K (2006) *Phys Rev Lett* 97:266802.
25. Aleiner IL, Efetov KB (2006) *Phys Rev Lett* 97:236801.
26. Altland A (2006) *Phys Rev Lett* 97:236802.
27. Ostrovsky PM, Gornyi IV, Mirlin AD (2006) *Phys Rev B* 74:235443.
28. Ando T, Fowler AB, Stern F (1982) *Rev Mod Phys* 54:437–672.
29. Efros AL, Pikus FG, Burnett VG (1993) *Phys Rev B* 47(4):2233–2243.
30. Galitski VM, Adam S, Das Sarma S (2007) *Phys Rev Lett*, in press.
31. Das Sarma S, Hwang EH (2003) *Phys Rev B* 68(19):195315.
32. Ilani S, Yacoby A, Mahalu D, Shtrikman H (2000) *Phys Rev Lett* 84(14):3133–3136.
33. Stauffer D, Aharony A (2001) *Introduction to Percolation Theory* (Taylor and Francis, Philadelphia).
34. Das Sarma S, Lilly MP, Hwang EH, Pfeiffer LN, West KW, Reno JL (2005) *Phys Rev Lett* 94(13):136401.
35. Allison G, Galaktionov EA, Savchenko AK, Safonov SS, Fogler MM, Simmons MY, Ritchie DA (2006) *Phys Rev Lett* 96(21):216407.
36. Tracy LA, Eisenstein JP, Lilly MP, Pfeiffer LN, West KW (2006) *Solid State Commun* 137:150–155.
37. Bardarson JH, Tworzydło J, Brouwer PW, Beenakker CWJ (2007) *Phys Rev Lett* 99:106801.
38. Nomura K, Koshino M, Ryu S (2007) *Phys Rev Lett* 99:146806.
39. Katsnelson MI (2006) *Eur Phys J B* 51:157–160.
40. Das Sarma S, Hwang EH (2004) *Phys Rev B* 69:195305.
41. Hwang EH, Das Sarma S (2007) *Phys Rev B* 75(20):205418.
42. Tworzydło J, Trauzettel B, Titov M, Rycerz A, Beenakker CWJ (2006) *Phys Rev Lett* 96(24):246802.
43. Fertig HA, Brey L (2006) *Phys Rev Lett* 97(11):116805.
44. Miao F, Wijeratne S, Zhang Y, Coskun U, Bao W, Lau CN (2007) *Science* 317:1530–1533.
45. Tan, Y.-W., Zhang Y, Bolotin K, Zhao Y, Adam S, Hwang EH, Das Sarma S, Stormer HL, Kim P (2007) *Phys Rev Lett*, in press.
46. Chen JH, Jang C, Fuhrer MS, Williams ED, Ishigami M (2007) arXiv:0708.2408.